Journal of Thermal Analysis and Calorimetry (2018) 133:951–960
https://doi.org/10.1007/s10973-018-7293-9

Highly stable copper/carbon dot nanofluid

Preparation and characterization

Zoha Azizi[1] · Abdolmohammad Alamdari[2] · Mohammad Mahdi Doroodmand[3]

Received: 31 January 2018 / Accepted: 7 April 2018 / Published online: 24 April 2018

Abstract
Copper/carbon dot nanohybrids (Cu/CD NHs) were prepared via a facile precipitation method through a disproportionation reaction. The surface characterization was performed by various techniques such as XRD, FTIR and TEM. Then, water-based nanofluids composed of Cu/CD NHs at 0.1 and 0.5 mass% were prepared, and their thermo-physical properties including thermal conductivity, viscosity, density and specific heat were evaluated at various temperatures. The water-based Cu/CD nanofluid demonstrated to be a potential heat transfer fluid with a high stability. It was found that the thermal conductivity can be enhanced by increasing the nanoparticle concentration and temperature. Almost 1.25-fold increase in thermal conductivity has been achieved by raising the temperature up to 50 °C and at the concentration of 0.5 mass%. The heat capacity was found to increase with increasing concentration. Moreover, by increasing temperature the density and viscosity of the as-prepared nanofluid decreased, whereas the heat capacity showed an increasing trend.

Keywords Nanohybrids · Carbon dot · Nanofluid · Disproportionation reaction · Thermal conductivity

Introduction

Nanofluids are the suspensions of nanomaterials, such as nanoparticles, nanofibers, nanotubes, nanowires, nanorods, nanosheets or droplets in a base fluid, and their specific properties offer potentials for many applications. The preparation of the nanofluid is commonly carried out by two methods of single-step and two-step [1].

Many researchers have recently reported the enhancement of convective heat transfer coefficient of various nanofluids in several channels and heat exchangers [2–12]. This enhancement was attributed to the enhancement of thermal conductivity, Brownian motion, thermo-phoresis, diffusion phoresis, and so on. In this regard, various studies have been carried out on the thermo-physical properties of different nanofluids [13–17]. On the other hand, the stability of nanofluids has always been a big challenge since the agglomeration tendency of the nanoparticles in the base fluid not only leads to the settlement and plugging problems, but also changes the physical properties of the nanofluid [1]. In this regard, various methods including pH control, addition of surfactants and sonication have been used to provide the stability of the nanofluids [18]. However, some constraints have been arising when such stabilized nanofluids were used as the working fluid in heat transfer devices, especially when a surfactant was added to maintain the nanofluid stability. Nanoparticles may lose their connections with the surfactant molecules at higher temperatures and hence may aggregate and collapse. Additionally, foaming of nanofluids in heat transfer devices was reported as another drawback of using surfactants [1].

Quantum dots (QDs) are nanoparticles of semiconductors usually employed in sensor applications because of their optical properties [19]. Carbon quantum dots, usually

✉ Zoha Azizi
azizi.zoha@gmail.com

✉ Abdolmohammad Alamdari
alamdari44@yahoo.com

[1] Department of Chemical Engineering, Mahshahr Branch, Islamic Azad University, Mahshahr, Iran

[2] Department of Chemical Engineering, School of Chemical and Petroleum Engineering, Shiraz University, Shiraz 7193616511, Iran

[3] Department of Chemistry, College of Sciences, Shiraz University, Shiraz 71454, Iran

referred to as carbon dots (CDs), mainly comprised of carbon and oxygen have recently received special attention for the biological applications. Unlike QDs of heavy metal, the CDs cause no toxicity or pollution to the environment [20]. Moreover, due to the high concentration of functional groups such as carboxyl group on the surface of CDs, they have excellent stability in aqueous solutions and also can be functionalized easily [21–23].

Nanohybrids (NHs) are the combination of two or more materials on the nanoscale, which offer multiple functionalities. The valuable achievements in synthesis of nanometals and semiconductors resulted in the development of metal-semiconductor NHs, which exhibited the combined and often synergistic properties [24]. Early instances of metal-semiconductor NHs are the growth of Cu, Au, Ag and Pt shells on ZnO cores [25].

CDs can easily be functionalized and used as NHs since they are capable of reducing metal salts [22, 23, 26]. Various techniques such as the chemical oxidation [27], the thermal cracking of organic compounds [28], the microwave-assisted hydrothermal synthesis [29], the rapid plasma pyrolysis [30], the alkali-assisted electrolysis of graphite [31] and various carbon precursors including graphite [32–35], graphene oxides [36–39], fullerene [40], carbon fibers [41] and organic carbon sources [42–46] have been used to prepare CDs. Owing to their excellent optical properties, thermal stability, chemical inertness and biocompatibility, CDs were employed in catalysis and energy-related fields [26]. Recently, they have been used as reducing and stabilizing agents in the synthesis of nanometals and effective catalysts [22, 23]. However, CDs are rarely used in the manufacture of nanofluids, and in particular, they have not been used in hybrids with other particles for heat transfer purposes according to our literature survey. A very novel research by Ettefaghi et al. [47] suggests that CDs have formed a very stable nanofluid, and its thermal properties in various concentrations have also been discussed. As mentioned previously, CDs can be employed as a reducing agent and are easily functionalized. Inspired by these capabilities, we have used CDs for the preparation of water-based Cu nanofluid, because they were capable of reducing the copper (I) and copper (II) ions to the copper (0), and simultaneously, a hybrid of copper supported on CDs was expected to be formed in the solution. Further, since CDs are stable in aqueous solutions [21–23], the dispersion of the Cu/CD NHs in water could also yield a stable nanofluid. Therefore, the aim of this report is to propose a method of preparation of Cu/CD NHs, followed by evaluating the thermo-physical properties thereof. The prepared Cu/CD nanofluid with a high stability can be used in thermal applications, without addition of any dispersant or surfactants. We believe that further progress of research on metal/carbon dot nanofluids leads to promising results in enhancement of heat transfer.

Materials and methods

Materials

All the chemicals were analytical grade and used as purchased without further purification. Copper (I) iodide, CuI, of 99% purity (Merck), was used as the precursor. Carbon dot previously synthesized by sonoelectrochemical exfoliation method [48] was utilized as reducing and stabilizing agent. Distilled water was used as the solvent. Sodium hydroxide (NaOH) and acetic acid (CH_3COOH, > 98%, China) were used to adjust the pH.

Synthesis of Cu/CD NHs

As mentioned previously, the copper nanoparticles are required to be protected from possible agglomeration, prior to their dispersion in water. For this purpose, inspired by the work of [22] the carbon dot is selected as a reducing and capping (protecting) agent in the stage of synthesis. It is expected that the Cu nanoparticles is formed while being capped by CDs through a disproportionation reaction.

Disproportionation reaction is a reaction in which oxidation and reduction of an element occur at the same time, leading to the production of two different substances [49]. By a typically reversible disproportionation reaction, the copper (I) ion produces both copper (II) and copper (0) through oxidation and reduction, respectively. However, as the electrochemical potential of the reaction presented in Eq. (1) is positive [50], the Cu (II) is more stable in the aqueous solution than Cu(I). Hence, the disproportionation reaction presented as Eq. (2) proceeds to the right.

$$\begin{aligned} &Cu^{2+}(aq) + e \rightarrow Cu^{+}(aq) \quad E^0 = 0.153\ V \\ &Cu^{+}(aq) + e \rightarrow Cu(aq) \quad E^0 = 0.521\ V \end{aligned} \tag{1}$$

$$\begin{aligned} &E^0 = 0.521 - 0.153 = 0.368\ V > 0 \\ &2Cu^{+}(aq) \leftrightarrow Cu^{2+}(aq) + Cu(s) \end{aligned} \tag{2}$$

To describe the synthesis method, first a suspension of CDs in water was prepared by a simple mixing of CDs powder (1 g) with water (100 mL). Then, a homogeneous mixture of copper iodide and water was prepared at a vigorously stirred condition. Due to its very low solubility in water, copper iodide (0.1 g CuI/(1 l water)) could easily make the distilled water supersaturated at 80 °C while vigorously stirred under reflux condition. After half an hour, the transparent solution changed to a milky one, and then the carbon dot suspension was added drop wise to the solution

at constant temperature of 80 °C. The mixture gradually turned into brown, then light yellow and finally dark yellow after the completion of the reaction (almost 8 h).

At the next stage, the suspension underwent three stages of annealing (warming up to 50 °C followed by cooling to the ambient temperature in each stage) in order to further strengthen the suspended nanoparticles. According to [24], this temperature treatment leads to a high-quality epitaxial interface between the metal and CDs. Finally, the sediments were removed by filtration under vacuum. The particles were collected by centrifugation at 4000 rpm for 20 min (Kobuta Model 6500), washed with ethanol for three times and dried in open air. Figure 1 shows the physical appearance and the reduction mechanism of the prepared Cu/CD nanohybrids.

It seems that the supersaturated solution of Cu^{+} proceeds with the nucleation, then formation of metallic Cu nanoparticles on carbon surface. In other words, Cu(s) which is produced from the disproportionation reaction finds CDs as appropriate sites for its heterogeneous nucleation and growth to form Cu/CD NHs.

Preparation of Cu/CD nanofluid

The two-step method was employed to prepare the Cu/CD nanofluid. To follow this procedure, certain amount of the prepared Cu/CD NHs was dispersed in distilled water using stirrer for almost 1 h to obtain a homogeneous suspension as the nanofluid. The Cu/CD nanofluid was prepared at two mass fractions of 0.1 and 0.5%. No further material including surfactant or dispersant was used in the process of the nanofluid preparation.

Characterization

A Shimadzu-FTIR-8300 spectrophotometer was used to collect spectra. The morphology of the nanoparticles was investigated via transmission electron microscopy (TEM, CM30-Philips). The phase composition and crystallinity of the products were characterized using an X-ray diffractometer (XRD, Bruker D8). The size distribution of the nanoparticles was obtained by particle size analyzer (Scatteroscope, Quidix Co). Zetasizer Nano ZS (Malvern Instruments Ltd, Malvern, UK) was used to perform the Zeta potential tests on the synthesized nanofluids by the Electrophoretic Light Scattering (ELS) technique. UV–Vis absorption was collected using a UV–Vis spectrophotometer (JENWAY-7315). Investigation of copper concentration in the suspension of Cu/CD NHs was carried out by Varian-SpectrAA 220/880 Zeeman Atomic Absorption.

Thermo-physical properties of the Cu/CD nanofluid such as thermal conductivity, density and viscosity were also experimentally measured. The KD2 Pro thermal conductivity meter (Decagon devices, Inc.) was used to measure the thermal conductivity with a maximum uncertainty of ± 2%. The density of the nanofluid was measured using portable DMA 35 N density meter (Anton Paar Co.) with an uncertainty of 0.0001 g cm^{-3}, and the viscosity was measured using Cannon–Fenske viscometer with an uncertainty of 0.001 cS.

Results and discussion

Infrared spectroscopic studies

The FTIR spectra of CDs and Cu/CD NHs are shown in Fig. 2. Comparing the two spectra, it is observed that the C–O stretching vibration at 1099 and 1261 cm^{-1} reduced to some extent, signifying the involvement of the carboxyl and carbonyl groups in the reduction process and subsequent action as a stabilizing agent where the metal surface is bound to the carboxylic moieties by coordination reactions [22]. However, the peak at 1373 cm^{-1} [51] indicated the increase of carboxyl groups. The peak at 594 cm^{-1} is attributed to the formation of Cu–O [23]. Other functional groups and chemical linkages of carbon dot (e.g., hydroxyl groups at 3400–3500 cm^{-1}, C–H vibration at 2850–2923 cm^{-1}, hydroxyl group at 1627–1635 cm^{-1}) [22, 23] remained intact after the formation of the

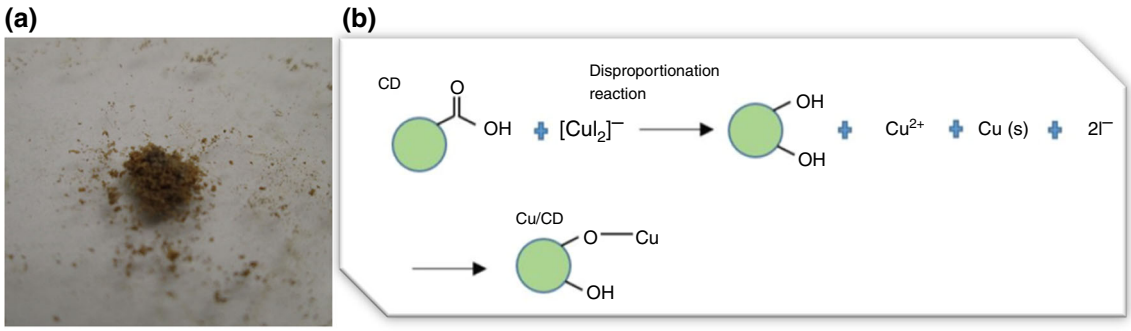

Fig. 1 **a** Physical appearance of the prepared Cu/CD NHs, **b** reduction mechanism for the preparation of Cu/CD NHs

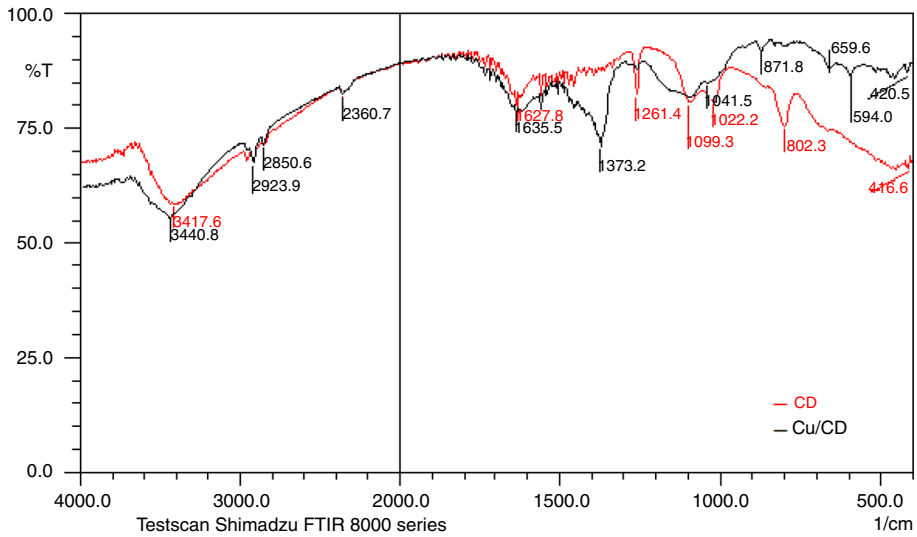

Fig. 2 FTIR spectra of CD and Cu/CD NHs

nanohybrid. The peripheral polar groups on the CDs also stabilize the Cu nanoparticles.

The abundant hydrophilic groups play an important role in stability of the Cu/CD in the aqueous solution, which is useful when the powder is dispersed in water to prepare the nanofluid for heat transfer purposes.

The physical structure of Cu/CDNHs

Figure 3 shows the TEM image of Cu/CD NHs, showing clearly that the as-prepared nanohybrids are quasi-spheres, and well dispersed particles having an average diameter of 20 nm. As demonstrated in the figure, the Cu nanoparticles appeared to form chain like structures embedded within a carbon matrix, suggesting that the growth of the nanoparticles was initiated from the CD surface [22]. The peripheral carboxyl groups presumably facilitated the binding and subsequent reduction of the metal salts. The SEM image is also presented in Fig. 3b, c, which shows the particle size is in the range of 10–60 nm.

Crystal phase of the products

The formation of Cu was confirmed through the XRD pattern of the nanohybrid (Fig. 4), using CuKα as a radiation source (λ=1.5406 Å). The samples were scanned in the 2θ range from 10° to 90° at a scanning rate of 5° min^{-1}. The peaks in Fig. 4 at 2θ (°) = 50.25 and 72.3 are corresponding to crystallographic spacing d200 and d220, respectively, which were found in accordance to other reports and JCPDF #78-2076 data for Cu nanoparticles [52, 53]. The average grain size of Cu/CD calculated by Scherrer's equation [54] was found to be around 20 nm, which agrees with the result of the particle size determined by TEM technique.

Particle size distribution (PSD)

Besides the mean particle size, the size distribution is the most important information obtained from the PSD data from which the broadness and the degree of asymmetry of size distribution are obtained [54]. The PSD results of the prepared nanofluids for both concentrations were almost the same, shown in Fig. 5. The figure indicates that the Cu/

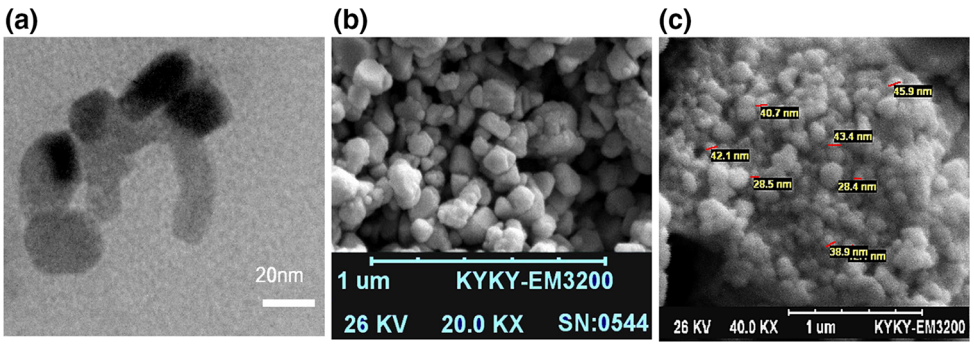

Fig. 3 **a** TEM image, **b**, **c** SEM images of Cu/CD NHs

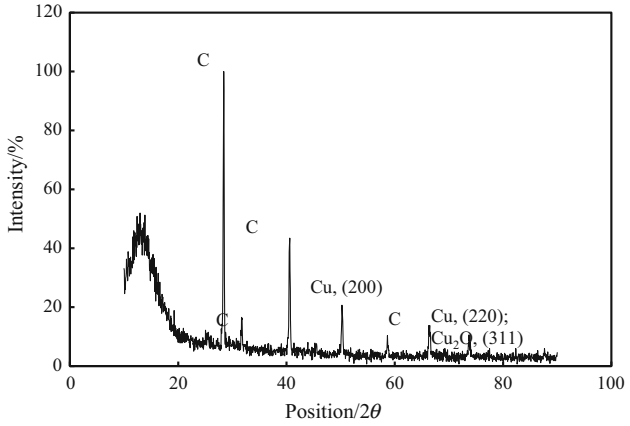

Fig. 4 XRD pattern for Cu/CD NHs

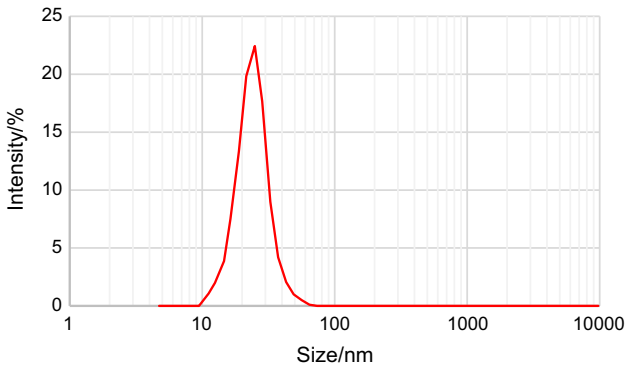

Fig. 5 Particle size distribution of Cu/CD nanofluid

CD NHs have a narrow size distribution centering at ca. 25 nm, with an average size of 25.7 nm. As illustrated, the distribution is almost symmetrical with a little broadness. Therefore, the as-prepared nanofluid is homogeneous from the particle size point of view.

Stability of Cu/CD nanofluid

Figure 6 shows the photograph of the as-prepared suspension of Cu/CD NHs; no sediments were found after 1 month being at a stationary state. This excellent stability of the suspension can be explained through the synthesis process. In the reduction process of Cu^{+} to form Cu^{0}, carbon dots not only act as the reducing agent, but also act as the stabilizing agent which can establish a good dispersion of generated nanohybrids. This is due to existence of a large number hydroxyl, carbonyl, carboxylic acid and epoxy groups on the surface of carbon dots, as previously reported by [48]. Therefore, utilizing the CD as the sites of nanoparticle growth can also provide an excellent stability for the nanofluid. Moreover, the peripheral polar groups, such as hydroxyl and aldehyde of carbon dots, helped to reduce Cu^{+} into Cu^{0}.

Fig. 6 The as-prepared Cu/CD suspension at 0.5 mass% after 1 month of stationary state

Apart from the stabilizing character of the CD, the dynamic nature of the suspension probably helped its high stability. According to HSAB theory, soft acids form stronger bonds with soft bases, whereas hard acids form stronger bonds with hard bases [55]. In the suspension under study, the soft base of I^{-} in combination with the soft acid of Cu^{+} formed a soft–soft interaction [56] resulting in the consumption of Cu^{+}. Consequently, regarding the disproportionation reaction Eq. (2), the reverse reaction proceeded. According to the positive electrochemical potential and at the same time the soft–soft interaction, the forward reaction proceeded at the same rate as the reverse reaction. Therefore, the possible agglomeration of the nanohybrids was prevented yielding a dynamically stable suspension.

Figure 7a shows the absorption spectra of CD (dispersed in water at 0.1 mass%) and Cu/CD nanofluids at 0.1 and 0.5 mass%. A narrow peak at 250 nm in the CD can be assigned to the π–π* transition of nanocarbon [57]. However, in the Cu/CD nanofluid, this characteristic peak disappeared.

Li et al. [54] studied the effect of some influencing parameters including pH on the stability of Cu nanofluid. A similar investigation was conducted to find the optimum pH for the present suspension using UV–visible spectroscopy (wavelength = 300 nm). The results of this analysis were recorded after 1 day in stationary state. The higher absorption shows the larger number of suspended nanoparticles in water, which indicates a higher stability for the nanofluid. Figure 7b shows the absorption against pH for a sample of Cu/CD nanofluid at a concentration of 0.1 mass%. According to the figure, the optimum pH to reach the stable nanofluid is 6.2.

The relative concentration is the ratio of the daily concentration of nanofluid to its initial concentration (in the

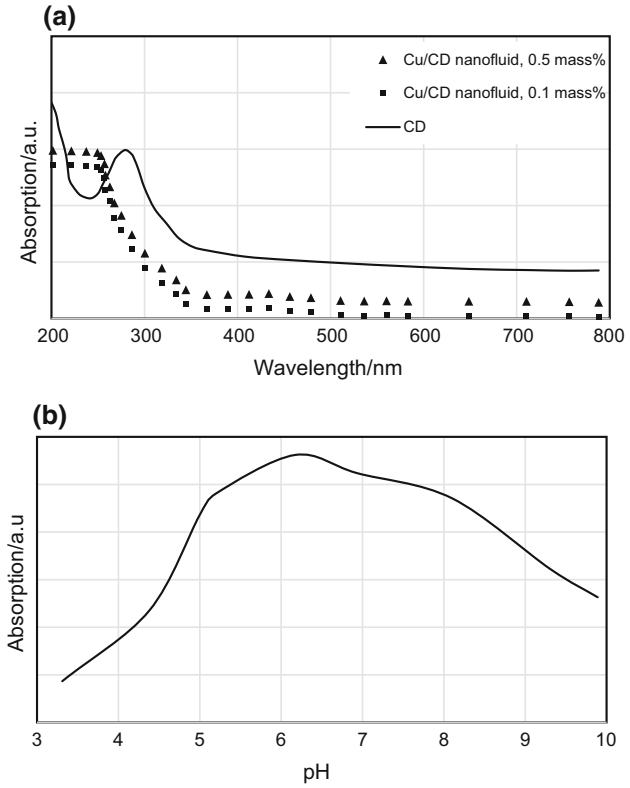

Fig. 7 UV/vis absorption spectra **a** of CD and Cu/CD nanofluids, **b** against pH for 0.1 mass% of Cu/CD nanofluid

fresh state), previously defined by [57]. To investigate the relative concentrations versus time in the present work, the mass concentration of the samples of Cu/CD nanofluids at 0.1 and 0.5 mass% were measured during a month and presented in Fig. 8. This figure shows that the Cu/CD nanofluids have a stable condition under UV–Vis irradiation. It is also inferred that after an initial decrease of the relative concentrations, it fluctuates, e.g., around 99.4 for 0.1 mass%. The maximum decreasing rate at the initial stage is around 7%.

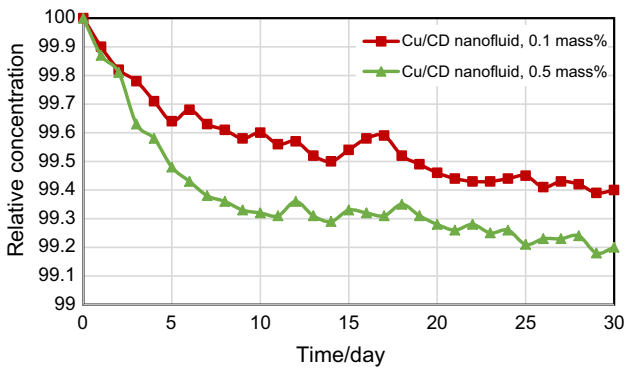

Fig. 8 Relative concentration versus time for Cu/CD nanofluids at 0.1 and 0.5 mass%

Zeta potential can also be used to identify the stability of a colloidal suspension [57]. The result of Zeta potential test is shown in Fig. 9. As can be seen, the Zeta potential value was found to be about-31.5 mV, indicating high stability of the Cu/CD nanofluid.

An atomic absorption analysis was also carried out to determine the concentration of various copper compounds present in the suspension. The two samples of 1000 mL volume of suspensions of nanohybrids (named s1 and s2) produced in water were subjected to this analysis. The concentrations of Cu/CD NHs were 0.1 and 0.5 mass% in s1 and s2, respectively. The unknown concentration related to Cu compounds was determined in terms of the carbon dot content of each sample. Results of the atomic absorption show that Cu content of the sample s1 is 52.10 mg(Cu)/g(CD) and that of s2 is 102.73 mg(Cu)/g(CD).

Effect of temperature on thermo-physical properties

The improving performance of the nanofluids in heat transfer devices is usually justified through the investigation of thermo-physical properties [58]. The thermo-physical properties may change in the heat transfer processes mainly due to their temperature dependency. In this research, the variations of density, viscosity, heat capacity and thermal conductivity with temperature were investigated for the Cu/CD nanofluid at two different concentrations of 0.1 and 0.5 mass%, shown in Fig. 10a–d.

According to Fig. 10a, b, the density as well as viscosity decreased with increasing temperature. Moreover, a four-fold increase in the viscosity was obtained by increase of the nanofluid mass fraction, while the impact of concentration variation on the density was not appreciable.

The variations of the heat capacity of the Cu/CD nanofluid against temperature were also investigated and compared with those reported by Barbes et al. [59] for CuO nanofluid (Fig. 10c). As shown in the figure, contrary to the

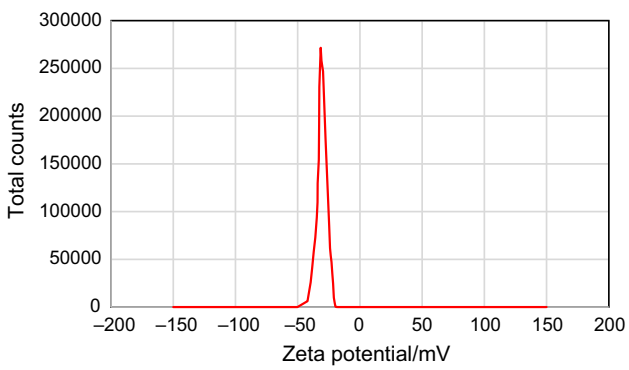

Fig. 9 Zeta potential of Cu/CD nanofluid at 0.5 mass% after 1 day

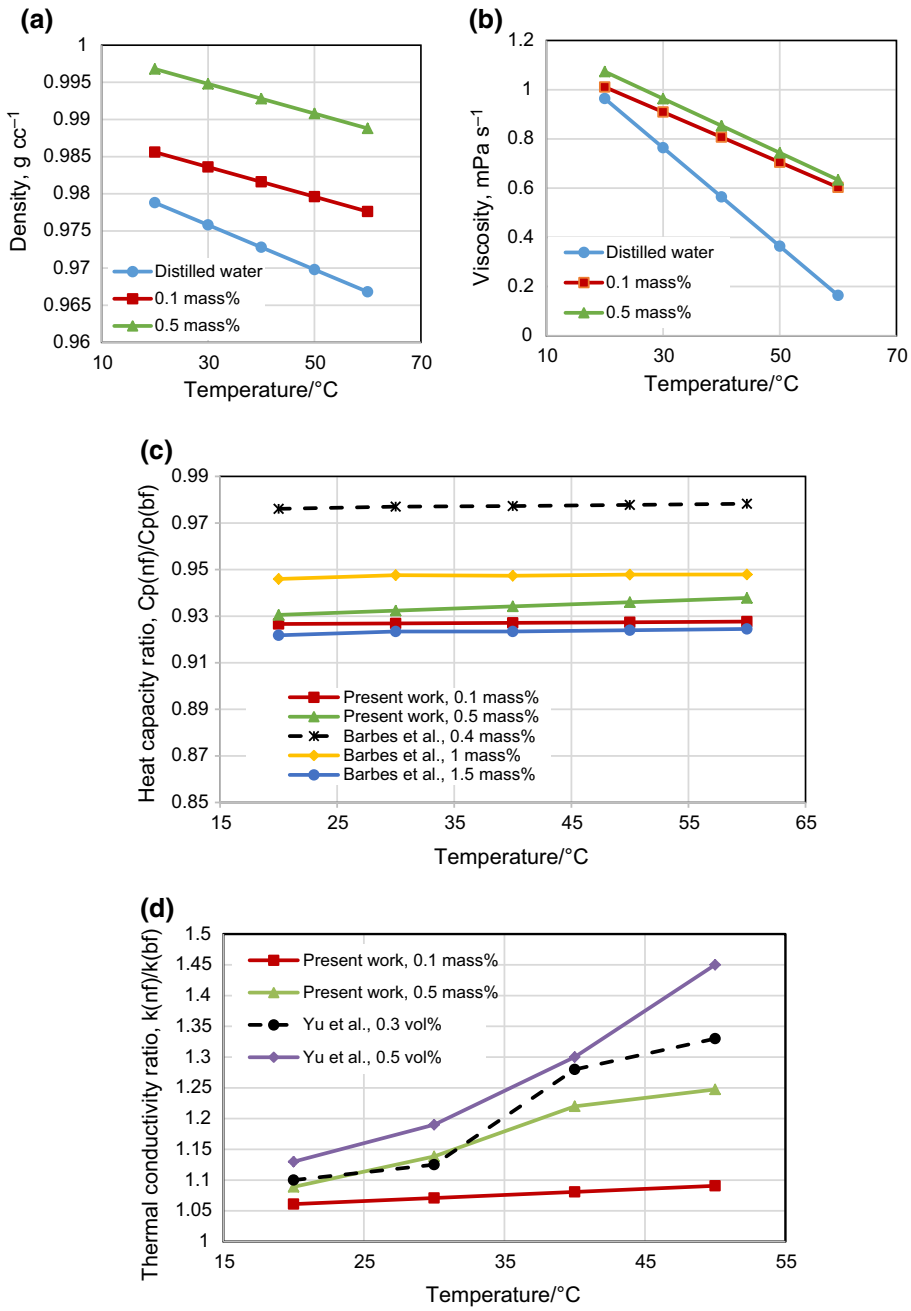

Fig. 10 Effect of temperature on **a** density, **b** viscosity, **c** heat capacity, **d** thermal conductivity of Cu/CD nanofluid at different nanohybrid concentrations

results presented by Barbes et al. [59], the heat capacity of the prepared nanofluid increased with concentration.

Among the reported studies on thermo-physical properties of nanofluids, the effect of the presence of nanoparticles on heat capacity of the base fluid does not yield a consistent result (e.g., [60–65]). There are several studies which report the strong and weak dependence of *Cp* on the volume fraction of nanoparticles. Yang et al. [66] reported that at low volume fraction and moderate temperature change, the heat capacity of nanofluid doesn't change much when compared to that of base fluid. Das and co-workers observed reduced specific heat capacities of a mixture of water and ethylene glycol by the addition of silicon dioxide, zinc oxide and alumina nanoparticles. They have reported the decrease of specific heat capacity of the nanofluid with increasing nanoparticle concentration [60–62]. Zhou and Ni [63] also found a reduced specific heat capacity of the water-based alumina. However, enhanced heat capacity of the nanofluid compared to that of base fluid was also reported in [67–69], for the particle mass concentration less than 1 mass% which was attributed to the existence of nanolayers surrounding the nanoparticles. Angayarkann et al. [70] reported that the specific heat capacity of Al_2O_3/PAO increased up to 4 mass%

nanoparticle concentration. Further increase in Al_2O_3 concentration led to a decrease in the Cp_{nf} but larger than the Cp_{bf}. These results suggest that PAO molecules strongly modify the interfacial thermal characteristics of Al_2O_3 nanoparticles that increases the heat capacity of PAO based Al_2O_3 nanofluids. They have discussed that this enhancement can be due to the additional thermal storage mechanisms caused by interfacial interactions between nanoparticle and the adhering liquid molecules, and the existence of semisolid–liquid layer adhering to the nanoparticles, which are likely to enhance the specific heat capacity due to the smaller intermolecular spacing similar to the nanoparticle lattice structure on the surface.

Also, regarding the results of [59], the impact of temperature on heat capacity of Cu/CD nanofluid at 0.5 mass% is comparatively considerable, and the heat capacity in the present work can be enhanced almost 0.7% by increasing the temperature up to 60 °C.

Thermal conductivity was also studied in terms of the ratio of thermal conductivity of the nanofluid to that of the distilled water (k_{nf}/k_b), shown in Fig. 10d. According to Yu et al. [71], thermal conductivity of the ethylene glycol-based nanofluid containing copper nanoparticles improves significantly with increasing temperature. For the present Cu/CD nanofluid, the (k_{nf}/k_{bf}) also increased, almost 25%, at temperature of 50 °C. There are various models in literature predicting the thermal conductivity referred to as effective thermal conductivity [72], but few of them concerned the effect of temperature. It is believed that the nanoparticles carry a relatively large volumes of the base fluid during their randomly movement in a quiescent suspension; and this effect known as Brownian motion is raised by the increase in temperature [73]. The data presented by Chon et al. also show that the Brownian motion is evidently a function of temperature especially for the smaller sizes of the nanoparticles [74]. The particle size of the present study is almost 25 nm; hence, the increase in thermal conductivity with temperature is expected.

Various models proposed for thermal conductivity of nanofluids show a link between k_{nf} and φ, the volume fraction of nanoparticles. Almost all of them indicate the ascending trend of thermal conductivity with increasing the nanoparticle concentration [75–78]. However, as shown in Fig. 10d, compared to Yu et al. [71] who reported an increase of up to 45% for the thermal conductivity using ethylene glycol-based copper nanofluid, it is observable that the corresponding value is only 25% at the same temperature in the present work. They prepared stable Cu-EG nanofluid by addition of the copper nanoparticles into 30 mL ethylene glycol with 1.5 g PVP as dispersant under ultrasonic oscillation for 30 min. The size of resulted copper nanoparticles ranged from 5 to 10 nm [71], which is less than the particle size of Cu/CD NHs in the present study. More importantly, the particle concentrations used in the present work are based on mass fraction, while Yu et al. [71] have introduced the volume fractions, and the corresponding mass fractions would be a higher value. Therefore, the lower thermal conductivity ratio in the present work shown in Fig. 10d can be attributed to the lower particle concentrations. Another factor which should be taken into account is the phenomenon of nanoparticle clustering, which plays an important role in improving the thermal conductivity of nanofluids. The low concentration of Cu/CD nanofluid may lead to decrease of nanoparticle clustering and the thermal conductivity ratio is subsequently reduced compared to the result of Yu et al. [71].

Moreover, a recent study on the synthesis and application of a graphene quantum dot nanofluid by Ettefaghi et al. [79] indicates that the thermal conductivity enhancement for a concentration of 0.1 mass% at ambient temperature is 5.7%, which agrees with our own result at the same temperature and concentration.

Conclusions

The main goal of the present work is to introduce quantum dots-based nanofluids with high stability, appropriate heat transfer properties accompanied by environmentally friendly and cost-effective characteristics which lead to energy conservation. Owing to the possible environmental risks caused by the use of surfactants as stabilizing agents for the preparation of heat transfer nanofluids, biocompatible CD is considered in the present research as a reducing, and at the same time-stabilizing agent. Therefore, Cu/CD nanohybrid with an average size of 25.7 nm was synthesized through growing the Cu nanoparticles on the surface of the CD. The water-based nanofluid containing nanohybrids of Cu/CD exhibited well dispersion and high stability in the absence of any stabilizer. The measurement of thermo-physical properties has revealed that temperature can affect the density, viscosity and thermal conductivity of the as-prepared nanofluid, and to a lesser extent, the heat capacity thereof. However, the heat capacity increased with increasing concentration. A 25% enhancement in thermal conductivity is also achieved by increasing the nanofluid concentration to 0.5 mass%. Due to the small size of Cu/CD nanohybrids, higher enhancement of thermal conductivity ratio (k_{nf}/k_{bf}) may be possible if the nanofluid is employed at higher temperatures and concentrations.

Acknowledgements The authors express their gratitude to Dr. Soheil Sayyahi (from Department of Chemistry, Mahshahr branch, Islamic Azad University, Mahshahr, Iran) for his valuable guidance.

References

1. Yu W, Xie H. A review on nanofluids: preparation, stability mechanisms, and applications. J Nanomat. 2012;2012(1):1–17.
2. Koo J, Kleinstreuer C. Laminar nanofluid flow in microheat-sinks. Int J Heat Mass Transf. 2005;48:2652–61.
3. Jang SP, Choi SUS. Cooling performance of a microchannel heat sink with nanofluids. Appl Therm Eng. 2006;26:2457–63.
4. Lee J, Mudawar I. Assessment of the effectiveness of nanofluids for single phase and two-phase heat transfer in micro-channels. Int J Heat Mass Transf. 2007;50:452–63.
5. Ho CJ, Wei LC, Li ZW. An experimental investigation of forced convective cooling performance of a microchannel heat sink with Al_2O_3/water nanofluid. Appl Therm Eng. 2010;30:96–103.
6. Bahiraei M, Rahim Mashaei P. Using nanofluid as a smart suspension in cooling channels with discrete heat sources. J Therm Anal Calorim. 2015;119(3):2079–91.
7. Hemmat Esfe M, Saedodin S. Turbulent forced convection heat transfer and thermophysical properties of Mgo–water nanofluid with consideration of different nanoparticles diameter, an empirical study. J Therm Anal Calorim. 2015;119:1205–13.
8. Azizi Z, Alamdari A, Malayeri MR. Convective heat transfer of Cu–water nanofluid in a cylindrical microchannel heat sink. Energ Convers Manage. 2015;101:515–24.
9. Barzegarian R, Aloueyan A, Yousefi T. Thermal performance augmentation using water based Al_2O_3-gamma nanofluid in a horizontal shell and tube heat exchanger under forced circulation. Int Commun Heat Mass Transf. 2017;86:52–9.
10. Pourfayaz F, Sanjarian N, Kasaeian A, Razi Astaraei F, Sameti M, Nasirivatan Sh. An experimental comparison of SiO_2/water nanofluid heat transfer in square and circular cross-sectional channels. J Therm Anal Calorim. 2017. https://doi.org/10.1007/s10973-017-6500-4.
11. Arabpour A, Karimipour A, Toghraie D. The study of heat transfer and laminar flow of kerosene/multi-walled carbon nanotubes (MWCNTs) nanofluid in the microchannel heat sink with slip boundary condition. J Therm Anal Calorim. 2017. https://doi.org/10.1007/s10973-017-6649-x.
12. Keshavarz Moraveji M, Barzegarian R, Bahiraei M, Barzegarian M, Aloueyan A, Wongwises S. Numerical evaluation on thermal–hydraulic characteristics of dilute heat-dissipating nanofluids flow in microchannels. J Therm Anal Calorim. 2018. https://doi.org/10.1007/s10973-018-7181-3.
13. Amani M, Amani P, Kasaeian A, Mahian O, Pop I, Wongwises S. Modeling and optimization of thermal conductivity and viscosity of $MnFe_2O_4$ nanofluid under magnetic field using an ANN. Sci Rep. 2017;7:17369.
14. Amani M, Amani P, Mahian O, Estellé P. Multi-objective optimization of thermophysical properties of eco-friendly organic nanofluids. J Clean Prod. 2017;166:350–9.
15. Mahian O, Kianifar A, Wongwises S. Dispersion of ZnO nanoparticles in a mixture of ethylene glycol-water, exploration of temperature-dependent density, and sensitivity analysis. J Clust Sci. 2013;24(4):1103–14.
16. Yiamsawas T, Dalkilic AS, Mahian O, Wongwises S. Measurement and correlation of the viscosity of water-based Al_2O_3 and TiO_2 nanofluids in high temperatures and comparisons with literature reports. J Disper Sci Technol. 2013;34(12):1697–703.
17. Hosseini SM, Safaei MR, Goodarzi M, Alrashed AAA, Nguyen TK. New temperature, interfacial shell dependent dimensionless model for thermal conductivity of nanofluids. Int J Heat Mass Transf. 2017;114:207–10.
18. Haddad Z, Hakan CA, Oztop F, Mataoui A. A review on how the researchers prepare their nanofluids. Int J Therm Sci. 2014;76:168–89.
19. Frasco MF, Chaniotakis N. Semiconductor quantum dots in chemical sensors and biosensors. Sensors. 2009;9:7266–86.
20. Faisal N, Liang W, Long-feng Z, Xiang-ju M, Feng-Shou X. Ascorbic acid assisted green route for synthesis of water dispersible carbon dots. Chem Res Chin Univ. 2013;29(3):401–3.
21. Li H, Kang Z, Liu Y, Lee ST. Carbon nanodots: synthesis, properties and applications. J Mater Chem. 2012;22:24230.
22. Dey D, Bhattacharya T, Majumdar B, Mandani S, Sharma B, Sarma TK. Carbon dot reduced palladium nanoparticles as active catalysts for carbon-carbon bond formation. Dalton Trans. 2013;42:13821–5.
23. De B, Voit B, Karak N. Carbon dot reduced Cu_2O nanohybrid/hyper branched epoxy nanocomposite: mechanical, thermal and photocatalytic activity. RSC Adv. 2014;4:58453–9.
24. Banin U, Ben-Shahar Y, Vinokurov K. Hybrid semiconductor-metal nanoparticles, from architecture to function. Chem Mater. 2014;26(1):97–110.
25. Wood A, Giersig M, Mulvaney P. Fermi level equilibration in quantum dot−metal nanojunctions. J Phys Chem B. 2001;105(37):8810–5.
26. Wu M, Wang Y, Wu W, Hu C, Wang X, Zheng J, Li Z, Jiang B, Qiu J. Preparation of functionalized water-soluble photoluminescent carbon quantum dots from petroleum coke. Carbon. 2014;78:480–9.
27. Liu H, Ye T, Mao C. Fluorescent carbon nanoparticles derived from candle soot. Angew Chem Int Ed. 2007;46(34):6473–5.
28. Rahy A, Zhou C, Zheng J, Park S, Kim MJ, Jang I, et al. Photoluminescent carbon nanoparticles produced by confined combustion of aromatic compounds. Carbon. 2012;50(3):1298–302.
29. Tang L, Ji R, Cao X, Lin J, Jiang H, Li X, et al. Deep ultraviolet photoluminescence of water-soluble self-passivated graphene quantum dots. ACS Nano. 2012;6(6):5102–10.
30. Wang J, Wang CF, Chen S. Amphiphilic egg-derived carbon dots: rapid plasma fabrication, pyrolysis process, and multicolor printing patterns. Angew Chem Int Ed. 2012;124(37):9431–5.
31. Li H, He X, Kang Z, Huang H, Liu Y, Liu J, et al. Water-soluble fluorescent carbon quantum dots and photocatalyst design. Angew Chem Int Ed. 2010;49(26):4430–4.
32. Kim S, Hwang SW, Kim MK, Shin DY, Shin DH, Kim CO, et al. Anomalous behaviors of visible luminescence from graphene quantum dots: interplay between size and shape. ACS Nano. 2012;6(9):8203–8.
33. Yang F, Zhao M, Zheng B, Xiao D, Wu L, Guo Y. Influence of pH on the fluorescence properties of graphene quantum dots using ozonation pre-oxide hydrothermal synthesis. J Mater Chem. 2012;22(48):25471–9.
34. Li L, Wu G, Yang G, Peng J, Zhao J, Zhu JJ. Focusing on luminescent graphene quantum dots: current status and future perspectives. Nanoscale. 2013;5(10):4015–39.
35. Liu WW, Feng YQ, Yan XB, Chen JT, Xue QJ. Superior microsupercapacitors based on graphene quantum dots. Adv Funct Mater. 2013;23(33):4111–22.
36. Liu F, Jang MH, Ha HD, Kim JH, Cho YH, Seo TS. Facile synthetic method for pristine graphene quantum dots and graphene oxide quantum dots: origin of blue and green luminescence. Adv Mater. 2013;25(27):3657–62.
37. Loh KP, Bao Q, Eda G, Chhowalla M. Graphene oxide as a chemically tunable platform for optical applications. Nat Chem. 2010;2(12):1015–24.
38. Pan D, Zhang J, Li Z, Wu M. Hydrothermal route for cutting graphene sheets into blue-luminescent graphene quantum dots. Adv Mater. 2010;22(6):734–8.
39. He W, Lu L. Revisiting the structure of graphene oxide for preparing new-style graphene-based ultraviolet absorbers. Adv Funct Mater. 2012;22(12):2542–9.

40. Lu J, Yeo PSE, Gan CK, Wu P, Loh KP. Transforming C60 molecules into graphene quantum dots. Nat Nanotechnol. 2011;6(4):247–52.
41. Peng J, Gao W, Gupta BK, Liu Z, Romero Aburto R, Ge L, et al. Graphene quantum dots derived from carbon fibers. Nano Lett. 2012;12(2):844–9.
42. Li H, He X, Liu Y, Huang H, Lian S, Lee ST, et al. One-step ultrasonic synthesis of water-soluble carbon nanoparticles with excellent photoluminescent properties. Carbon. 2011;49(2):605–9.
43. Xu J, Zhou Y, Liu S, Dong M, Huang C. Low-cost synthesis of carbon nanodots from natural products as fluorescent probe for the detection of ferrum (III) ion in lake water. Anal Methods. 2014;6(7):2086–90.
44. Liang Q, Ma W, Shi Y, Li Z, Yang X. Easy synthesis of highly fluorescent carbon quantum dots from gelatin and their luminescent properties and applications. Carbon. 2013;60:421–8.
45. Sun D, Ban R, Zhang PH, Wu GH, Zhang JR, Zhu JJ. Hair fiber as a precursor for synthesizing of sulfur-and nitrogen-co-doped carbon dots with tunable luminescence properties. Carbon. 2013;64:424–34.
46. Jia X, Li J, Wang E. One-pot green synthesis of optically pH sensitive carbon dots with up conversion luminescence. Nanoscale. 2012;4(18):5572–5.
47. Ettefaghi E, Rashidi A, Ghobadian B, Najafi G, et al. Experimental investigation of conduction and convection heat transfer properties of a novel nanofluid based on carbon quantum dots. Int Commun Heat Mass Transf. 2018;90:85–92.
48. Doroodmand MM, Mehrtash M. Selective synthesis of graphene quantum dots, carbon nanodots and their hybrids by sonoelectrochemical exfoliation method. J Nanoeng Nanomanuf. 2015;5(1):1–10.
49. Dj Safarik. Eldridge RB. Olefin/paraffin separations by reactive absorption: a review. Ind Eng Chem Res. 1998;37:2571–81.
50. Ebbing DD. General chemistry. 5th ed. Boston: Houghton Mifflin; 1996.
51. Silverstein RM, Bassler GC, Morrill TC. Spectrometric identification of organic compounds. 8th ed. New York: Wiley; 2014.
52. Kalidindi SB, Sanyal U, Jagirdar BR. Nanostructured Cu and Cu@Cu_2O core shell catalysts for hydrogen generation from ammonia-borane. Phys Chem Chem Phys. 2008;10:5870–4.
53. He P, Shen X, Gao HJ. Size-controlled preparation of Cu_2O octahedron nanocrystals and studies on their optical absorption. Colloid Interface Sci. 2005;284:510–5.
54. Li X, Zhu D, Wang X. Evaluation on dispersion behavior of the aqueous copper nano-suspensions. J Colloid Interf Sci. 2007;310:456–63.
55. Koch EC. Acid–base interactions in energetic materials: I. The hard and soft acids and bases (HSAB) principle-insights to reactivity and sensitivity of energetic materials. Propellants, Explos, Pyrotech. 2005;30(2):5–16.
56. Lefèvre G, Walcarius A, Ehrhardt JJ, Bessière J. Sorption of iodide on cuprite (Cu2O). Langmuir. 2000;16:4519–27.
57. Amiri A, Shanbedi M, Dashti H. Thermophysical and rheological properties of water-based graphene quantum dots nanofluids. J Taiwan Inst Chem Eng. 2017;76:132–40.
58. Azizi Z, Alamdari A, Malayeri MR. Thermal performance and friction factor of a cylindrical microchannel heat sink cooled by Cu-water nanofluid. Appl Therm Eng. 2016;99:970–8.
59. Barbes B, Paramo R, Blanco E, Casanova C. Thermal conductivity and specific heat capacity measurements of CuO nanofluids. J Therm Anal Calorim. 2014;115:1883–91.
60. Namburu PK, Kulkarni DP, Dandekar A, Das DK. Experimental investigation of viscosity and specific heat of silicon dioxide nanofluids. Micro Nano Lett. 2007;2:67–71.
61. Kulkarni DP, Vajjha RS, Das DK, Oliva D. Application of aluminum oxide nanofluids in diesel electric generator as jacket water coolant. Appl Therm Eng. 2008;28:1774–81.
62. Vajjha RS, Das DK. Specific heat measurement of three nanofluids and development of new correlations. J Heat Transf. 2009;131:071601.
63. Zhou SQ, Ni R. Measurement of the specific heat capacity of water-based Al_2O_3 nanofluid. Appl Phys Lett. 2008;92:093123.
64. O'Hanley H, Buongiorno J, McKrell T, Hu LW. Measurement and model validation of nanofluid specific heat capacity with differential scanning calorimetry. Adv Mech Eng. 2012;4:181079.
65. Sekhar YR, Sharma KV. Study of viscosity and specific heat capacity characteristics of water-based Al_2O_3 nanofluids at low particle concentrations. J Exp Nanosci. 2015;10:86–102.
66. Yang Y, Zhang ZG, Grulke EA, Anderson WB, Wu G. Heat transfer properties of nanoparticle-in-fluid dispersions (nanofluids) in laminar flow. Int J Heat Mass Transf. 2005;48:1107.
67. Hentschke R. On the specific heat capacity enhancement in nanofluids. Nanoscale Res Lett. 2016;11(1):88–99.
68. Shin D, Banerjee D. Enhancement of specific heat capacity of high-temperature silica-nanofluids synthesized in alkali chloride salt eutectics for solar thermal-energy storage applications. Int J Heat Mass Transf. 2011;54:1064–70.
69. Nelson IC, Banerjee D, Ponnappan R. Flow loop experiments using polyalphaolefin. J Thermophys Heat Transf. 2009;23:752–61.
70. Angayarkanni SA, Sunny V, Philip J. Effect of nanoparticle size, morphology and concentration on specific heat capacity and thermal conductivity of nanofluids. Nanofluids. 2015;4(3):302–9.
71. Yu W, Xie H, Chen L, Li Y. Investigation on the thermal transport properties of ethylene glycol-based nanofluids containing copper nanoparticles. Powder Technol. 2010;197:218–21.
72. Salman BH, Mohammed HA, Munisamy KM, Kherbeet A. Characteristics of heat transfer and fluid flow in microtube and microchannel using conventional fluids and nanofluids: a review. Renew Sust Energ Rev. 2013;28:848–80.
73. Koo J, Kleinstreuer CA. New thermal conductivity model for nanofluids. J Nanopart Res. 2004;6:577–88.
74. Chon SUS, Kihm CH, Lee Kenneth D, Choi SP. Empirical correlation finding the role of temperature and particle size for nanofluid (Al_2O_3) thermal conductivity enhancement. Appl Phys Lett. 2005;87:153107.
75. Prasher R, Bhattacharya P, Phelan PE. Thermal conductivity of nanoscale colloidal solutions (nanofluids). Phys Rev Lett. 2005;94(2):025901.
76. Jung JY, Yoo JY. Thermal conductivity enhancement of nanofluids in conjunction with electrical double layer (EDL). Int J Heat Mass Transf. 2009;52:525–8.
77. Jang SP, Choi SUS. Role of Brownian motion in the enhanced thermal conductivity of nanofluids. Appl Phys Lett. 2004;84(21):4316–8.
78. Barzegarian R, Moraveji MK, Aloueyan A. Experimental investigation on heat transfer characteristics and pressure drop of BPHE (brazed plate heat exchanger) using TiO_2–water nanofluid. Exp Thermal Fluid Sci. 2016;74:11–8.
79. Ettefaghi E, Ghobadian B, Rashidi A, Najafi G, et al. Preparation and investigation of the heat transfer properties of a novel nanofluid based on graphene quantum dots. Energ Convers Manag. 2017;153:215–23.